

Plant-extract-assisted green synthesis of silver nanoparticles using *Macaranga Indica* bark extract for antimicrobial and photocatalytic activity

G. Hegde^{1,3}, S. Yallappa^{2*}, T. Khadre³, Sudha Joseph⁴, J. Manjanna⁵

1. Environmental Lab, Indian Institute for Human Settlements, Bengaluru-560060, Karnataka, India
- 2*.Department of Chemistry, AMC Engineering College, Bangalore-560083, Karnataka, India.
- 3.Department of Chemistry, Dr. A.P.J Abdul Kalam University, Indore-452010, Madhya Pradesh, India
4. Department of Mechanical Engineering, Cambridge Institute of Technology, Bangalore 560036, Karnataka, India
5. Dept. of Chemistry, Rani Channamma University, Belagavi 591156, Karnataka, India

Email: yallappashiralgi5@gmail.com (S. Yallappa)

Received: 24.3.23, Revised: 27.4.23 Accepted: 28.4.23

Abstract: A rapid and environment-friendly green synthesis of silver nanoparticles (AgNPs) using *Macaranga Indica* (*M. Indica*) plant extracts was explored in this study. The obtained AgNPs were characterized by UV–Vis, XRD, FTIR, and SEM for antimicrobial and photocatalytic activities. The typical surface plasmon resonance peak around 440 nm confirmed the formation of AgNPs. The particles were found to be very tiny in the range of 15–20 nm size and showed *fcc* crystal symmetry. The FT-IR study showed the presence of bio-molecules on the surface of AgNPs and acting as capping agents. The *in vitro* antibacterial screen of AgNPs showed the bio-capped AgNPs have a higher inhibitory action for *E. coli* and *S. aureus* followed by *C.albicans*. The degradation property of the AgNPs towards Rhodamine B (RhB) under different conditions revealed that the degradation efficiency of phytochemicals-coated AgNPs on RhB was found to be high and around 88.8% within 70 min.

Key Words: AgNPs, *Macaranga Indica*, Rhodamine B, Antimicrobial activity

Introduction

M. indica has been traditionally used in Indian Ayurvedic and Siddha medicine to treat anemia, paralysis, tumors, cuts, wounds, colon cancer, and other related ailments¹⁻³. Plants of this genus have been reported to produce a range of phenolic compounds, most notably prenylated flavonoid and stilbenes⁴. *M. indica* is a species of tree that grows to about 25 meters in height. Previous phytochemical studies on *M. indica* led to the isolation and identification of flavonoids, isoflavones and their prenylated derivatives^{1, 5}. Although plant extracts are used in traditional medicine, the lack of sustained potency of the extract becomes a major obstacle in drug development⁶, hence new methods are required. Bio-inspired AgNPs offer mutation-resistant antibacterial properties and are used as filters in water treatment plants, wound healing ointments, HIV prevention and treatment, food packaging, cosmetic products as well as coatings on medical devices⁷⁻⁹. Different plant extracts derived from the leaves, bark, seeds, flowers, and fruits have demonstrated various advantages as both reducing and capping agents¹⁰⁻¹². Phytochemicals, the bioactive components of the plant extract are known for their role in reducing Ag⁺ ions and stabilizing NPs over a long period of time increasing biological and environmental applications.

In recent years, photocatalysis has been viewed as an alternative, cost-effective method to eliminate hazardous chemicals¹³. The photocatalytic process for breaking down organic pollutants has attracted a great deal of interest due to its exceptional advantages. Therefore, it is imperative to find a suitable and effective photocatalyst during the degradation process. The performance of a photo decolorization reaction is affected by the quality and properties of the photocatalyst, which is typically a semiconducting material with the ability to generate electron-hole pairs in the presence of light^{14, 15}. There were no reports on the biosynthesis of AgNPs using the aqueous bark extract of *M. Indica* which is a traditionally used ethnomedicinal plant as described here. The objective of the present work is to synthesize AgNPs by a green approach using the medicinally important *M. Indica* plant and to screen for bacterial and fungal activity against *E. coli*, *S. aureus*, and *C. albicans*. Moreover, the application of synthesized Ag NPs in photocatalytic degradation of RhB dye under UV light irradiation was investigated. The rate constant in photocatalytic degradation with respect to RhB dye concentration was also estimated. The rhodamine B is a toxic dye

widely used in traces and colorants, and is carcinogenic and mutagenic to humans and organisms. Microplastics can accumulate with RhB in the aquatic system leading to high environmental risks. Hence, it is necessary to remove it from the aquatic system by using sustainable methods.

2. Experimental

2.1. Materials

M. Indica bark was collected from the village of Siddapur Taluk, Bilgi in Karnataka, India in the Western Ghats. Hi-media Laboratory supplied analytical grade silver nitrate (AgNO_3) (Mumbai, India). The *M. indica* extract was prepared in distilled water using a microwave oven (LG MJEN326UH, 2.45 GHz) for subsequent AgNPs synthesis.

2.2. Green synthesis of AgNPs

To extract the phytochemicals, 6 g of freshly chopped, finely ground *M. Indica* bark was mixed with 250 mL of distilled water in a beaker. The mixture was then microwave-irradiated for around 300 seconds. In a heated environment, it was filtered using a 0.45-micron membrane filter. After cooling to room temperature (RT), it was used for the synthesis of AgNPs. In a typical synthesis of AgNPs, 50 mL of a 0.001M aqueous solution of AgNO_3 was mixed with 20 mL of bark extract. The mixture was exposed to microwave radiation for different intervals of time. The pale yellow to dark brown colour within 300 seconds indicates the formation of AgNPs. The prepared solution was stored for two days prior to characterization.

2.3. Characterization of solid AgNPs

The UV-vis spectra were recorded with a UV-Vis spectrometer (UV-2450, Shimadzu). The size and morphology of AgNPs were investigated using scanning electron microscopy (SEM) (JEOL-JSM 6701-F, Japan) operated at an accelerated voltage of 200 kV. The elemental composition was determined using the EDX analysis. With $\text{Cu-K}\alpha$ radiation from 10° to 60° (2θ) with a step size of 0.01° , the X-ray diffraction patterns were recorded with an X-ray diffractometer (D8 Focus, Bruker, Germany). To identify the potential biomolecules capping on AgNPs, an FTIR (Perkin Emler) spectrum was obtained in the KBr pellet.

2.4. *In vitro* antimicrobial activity AgNPs

The *in vitro* antibacterial activity of AgNPs was evaluated using the agar well diffusion method as follows¹⁶. Test pathogens included *E. coli* (ATCC 25922), *S. aureus* (ATCC 11682), and *C. albicans* (MTCC 3017). Mueller Hinton Agar (MHA) and Potato Dextrose Agar (PDA) were used for antimicrobial assays. A cork borer was used to create 6mm wells in the agar plates. In the wells, 100µL of AgNPs (50 µg/mL) were added. Ciprofloxacin and fluconazole were used as standards for both antibacterial and antifungal activity, respectively. Dimethyl sulfoxide (DMSO) was used as a control. The bacterial plates were incubated at 37 °C for 24 hours, while the fungal plates were incubated at 30 °C for 48 hours. The zone of inhibition (ZOI) was observed with a measuring scale after the incubation period. All tests were performed in triplicate.

2.5. Photocatalytic activity of green synthesized AgNPs

The photocatalytic activity of the green synthesized AgNPs was studied for the RhB dye under sunlight irradiation. To every 80 mg/L solution of the dye, 5 mg AgNPs were added and stirred in the dark for 30 min to reach adsorption/desorption equilibrium. Then, the reaction was moved outside to be carried out under sunlight. The progress of their action was monitored by measuring the absorbance of the reaction mixtures at intervals of 10, 20, 30, 40, 50, 60 and 70 mins after the initiation of the reaction under sunlight. The dye adsorption percentage is calculated using the following formula:

$$\% \text{ of RhB dye adsorption} = \frac{\text{Initial absorption} - \text{Final absorption}}{\text{Initial absorption}} \quad (1)$$

3. Results and Discussion

3.1. Green synthesis and characterization of AgNPs

After 10-300 seconds of microwave irradiation, the reaction mixture (50 mL of 1 mM AgNO₃ plus 20 mL of bark extract) changed color from pale yellow to black in about 60 seconds. With increasing irradiation time, the intensity of the reaction mixture increased until it reached saturation in about 300 seconds. The broad peak occurring in the region of 430–440 nm (Fig. 1a) depending on the exposure time is considered to be the Surface Plasmon Resonance (SPR) of AgNPs¹⁷. The inset of the figure shows the photocopy of the color of the

aqueous bark extract and AgNPs formation. This finding demonstrates that *M. Indica* bark extract reduces Ag^+ to Ag^0 . The increase in particle size and yield of AgNPs with irradiation time is likely the reason for the redshift of SPR from 430 nm to 450 nm. A similar UV-Visible spectrum was observed for AgNPs synthesized from *Cucumis prophetarum* aqueous leaf extract¹⁸ and *Cannabis sativa* leaf extract¹⁹.

The optical band gap of synthesized AgNPs was calculated according to the Tauc relation (ahv) is 2.8 eV.

$$ahv = A(hv - E_g)n \quad (2)$$

where α is the absorption coefficient, A is constant, ν is the frequency, h is the plank's constant, E_g is bandgap energy, and $n = 1/2$ is for a direct bandgap of the NPs. Fig. 1b shows an SEM image of as-synthesized AgNPs. The majority of bio-capped AgNPs are spherical, mono-dispersed particles with a diameter (ϕ) of between 15 and 20 nm. The SEM image shows a type of foam on the particles, which is most likely the result of the bio-capping of organic moieties from the plant extract. The EDX profile (Fig.1c) confirmed the presence of Ag as the main element with 53.47 atomic %. Traces of C, O, and Cl are also seen due to the presence of plant residue and other organic materials with AgNPs acting as bio-capping. The AgNPs are stabilized by bio-capping, and these bio-capping AgNPs, especially in combination with pharmacological plant extracts, have shown improved biological and photocatalytic activity^{20, 21}. The putative bio-molecules of *M. indica* bark extract involved in $AgNO_3$ reduction and AgNPs stabilization were identified by FTIR spectroscopy. The FTIR spectrum in Fig. 1(d) shows the major bands at 3265, 2935, 1568 and 1288cm^{-1} . The bands at 3265cm^{-1} and 2935cm^{-1} correspond to the OH stretch of the polyphenols group and the C-H stretching of the methylene group or a characteristic peak of triterpenoid saponins²². The bands at 1568cm^{-1} and 1288cm^{-1} may be assigned to the C-H bending of the aromatic and the C-N stretching of the amine group or the OH bending of the phenol respectively. A band appears at 1708cm^{-1} corresponding to C=O bond formation²³. This could be due to the oxidation of the OH group to the CO group⁸. This further indicates the role of polyphenolic compounds and proteins in the reduction of Ag^+ to Ag^0 . The capping of the AgNPs by the bio-molecules is also evident from the presence of the major bands in FTIR spectra. A typical XRD pattern of synthesized AgNPs is shown in the inset of Fig. 2. All peaks in the XRD pattern can be indexed as a face-centered cubic (*fcc*) structure of Ag (JCPDS No. 89-3722)²⁴. The XRD pattern shows the presence of diffraction peaks corresponding to (111), (200), (220), (311), and (331) planes. The mean particle size determined using the Scherrer

method at the prominent (111) diffraction peak is 18 ± 3 nm, agreeing with the size of isolated NPs observed in the SEM analysis.

3.2. Antimicrobial Activity of AgNPs

The bio-molecules coated AgNPs were tested for antibacterial activity against Gram-positive bacteria, Gram-negative bacteria, and a fungus. An antimicrobial test was carried out using the agar well diffusion assay²⁵ and the results showed high antimicrobial activity of AgNPs against all tested pathogens. **Table 1** shows the results for the mean zone of inhibition (ZOI) and minimum inhibitory concentration (MIC) for all pathogens tested. The MIC is the lowest concentration of drug that prevents visible microbial growth. The negative control, DMSO, showed no zone of inhibition. According to the ZOI, Gram-negative bacteria have the greatest antibacterial activity. The crude plant extract of *M. indica* showed very little inhibitory activity against the pathogens tested. Using broth dilution methods, the MIC for AgNPs is determined to be most effective against *E. coli*, followed by *S. aureus* and *C. albicans* (Fig. 3a). ZOI and MIC indicate that AgNPs restrict the development of both bacteria and fungi. The percentage of colonies formed on agar plates as a function of AgNPs concentration is shown in Fig. 3b. After treatment with AgNPs, it was found that the number of colonies decreased significantly compared to the control. A substantial peptidoglycan layer in the cell wall of *S. aureus* is responsible for the organism's low susceptibility²⁶.

Table 2 shows a comparison of the antibacterial activity of AgNPs synthesized using *M. indica* bark extract with that of previously reported studies. The MIC results of AgNPs synthesized with *Banana peel extract* are lower than those observed for AgNPs synthesized from *M. indica*, while the MIC of *Solanum tricobatum* and *Terminalia arjuna* bark extract are comparable to our results²⁷⁻²⁹. This demonstrates that AgNPs synthesized from *M. indica* exhibit superior antibacterial and antifungal activity. The antimicrobial activity, dispels the notion that cell membrane communication is caused by electrostatic interactions^{33, 34}. The size and shape of NPs are considered important parameters of antimicrobial activity. AgNPs accumulate in different parts of the cell and make the membranes of Gram-positive bacteria, Gram-negative bacteria and fungi less stable. This leads to cell lysis via the formation of pits and the accumulation of NPs in the cytoplasm. Furthermore, AgNPs having 20 nm size or smaller have more contact with cells than larger NPs leading to the internalization of NPs into cells and then the release of toxic ions²⁹. Thus, the size of the NPs is an important parameter for their antimicrobial activities and the better antimicrobial activity of AgNPs synthesized from *M. Indica* could be attributed to their small size.

3.3. Photocatalytic Activity of AgNPs

Rhodamine B (RhB) is a popular water-soluble dye widely used in industrial sectors such as textile, leather, printing, paper and pharmaceuticals. The degradation of this dye in the presence of green synthesized AgNPs was monitored with a UV–Vis spectrophotometer. The highest absorption of RhB was observed at 663 nm. The degradation of RhB dye upon solar irradiation catalyzed by AgNPs is reflected by a gradual decrease in the absorption peak of the dye solutions. From Fig. 4a it can be seen that the absorption band of RhB at 663 nm decreases with time and eventually approaches the baseline, indicating the successful degradation of the dye in the presence of AgNPs. Fig. 4(b) shows the variation of the $\ln(A_0/A_t)$ Vs time for RhB. The degradation rate constant calculated for RhB is $30 \times 10^{-3} \text{ min}^{-1}$. The decrease in $\ln(A_0/A_t)$ value with time indicates that the reaction process followed pseudo-first-order kinetics.

In this study, the percentage of RhB dye degradation calculated from the absorption spectra was 88.8%. Previous studies have reported that AgNPs synthesized using the solid-state thermal decomposition method achieved 40% RhB degradation after 60 min of sunlight exposure³⁵. Furthermore, Roy et al. observed that 75% of methyl orange dye was degraded in 480 minutes by AgNPs derived from *Solanum tuberosum* infusion³⁶. Liang et al. reported that no significant orange G dye degradation activity was observed using AgNPs prepared from *Lemon* fruit extract³⁷. This evidence conclusively shows that the AgNPs synthesized from *M. indica* extract in the present study exhibit stronger photocatalytic activity than AgNPs synthesized from other sources.

Since there are more active sites on the larger surface area of NPs, a wider variety of dye molecules can be degraded by electron transfer. Fig. 4c shows the mechanistic view of dye degradation in the presence of AgNPs. When exposed to Sunlight, the electrons in Ag ions become excited and transfer from the valence band to the conduction band. This creates electron-hole pairs that serve as effective oxidizing and reducing agents. These excited electrons generate free radicals such as $\text{HO}\cdot$, $\text{O}_2^{\cdot-}$ and $\text{HOO}\cdot$ on the catalyst surface, the active sites of AgNPs when they combine with the oxygen present in the reaction mixture³⁸. The rate of degradation is significantly influenced by the structure of the dyes and the structure of the polycyclic dyes used in this study as shown in Fig. 4c. The rate of dye degradation is slowed down by the presence of sulfonyl and nitro groups. Since RhB dye does not have a sulfonyl group, it degrades faster. It is imperative that the catalyst is reusable.

As a result, AgNPs obtained from *M. indica* bark extract were collected after each run and reused five times to determine their potency after each run. As shown in Fig. 4d, the activity of the catalyst slightly decreased after it was successfully used three times. For instance, up to three times the degradation of the catalyst was 88%, then the 4th run was reduced to 86.5% degradation and the 5th run was further reduced to 86 % degradation. This result demonstrates that AgNPs can be successfully recovered and reused, making them suitable for wastewater treatment.

4. Conclusion

AgNPs were synthesized by plant extraction-assisted green synthesis using *M. indica* bark extract and microwave irradiation technique. The synthesized AgNPs were characterized using UV-Vis spectrophotometer, SEM, EDX, XRD and FT-IR techniques and concluded that the formed AgNPs range in size from 15-20nm. The *in situ* coating with secondary plant substances is evident from the FTIR spectra. Phytochemical-coated AgNPs showed potent antimicrobial activity against *E. coli*, *S. aureus* and *C. albicans*. Adsorption studies with RhB dye have shown that AgNPs are able to remove 88.8 % of the dye within 70 min contact time. Overall, this work presents an environmentally friendly method for the rapid synthesis of AgNPs that can be used as antimicrobial agents and for treating wastewater.

Figures:

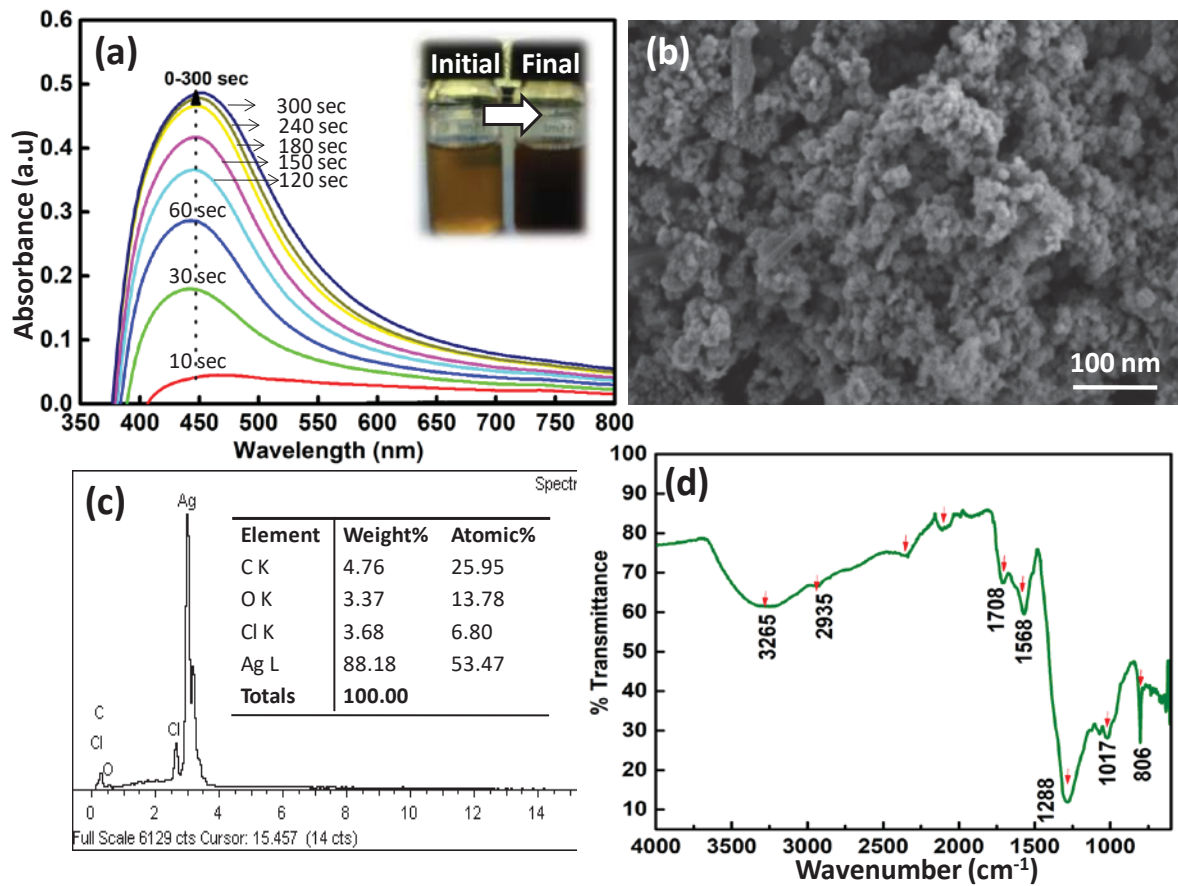


Fig. 1. (a) UV-Vis spectra of AgNPs formation at a different time interval (0-300 sec): insets hows the reaction mixture with *M. indica* bark extract at 10 and 300 seconds, (b) SEM image of AgNPs (c) EDX profile of AgNPs and (d) FTIR analysis of AgNPs.

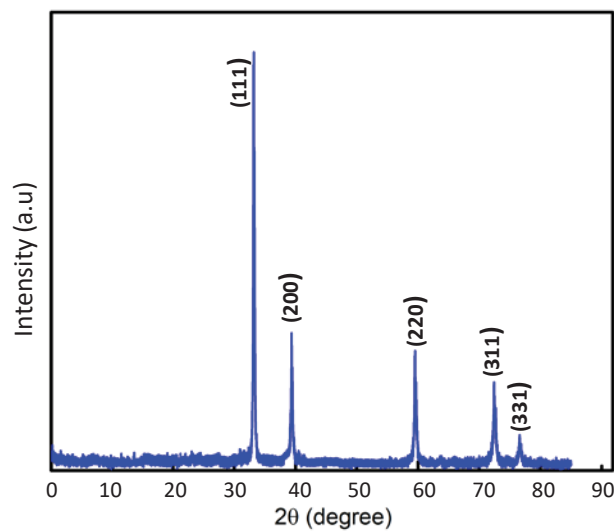


Fig. 2. XRD pattern of AgNPs

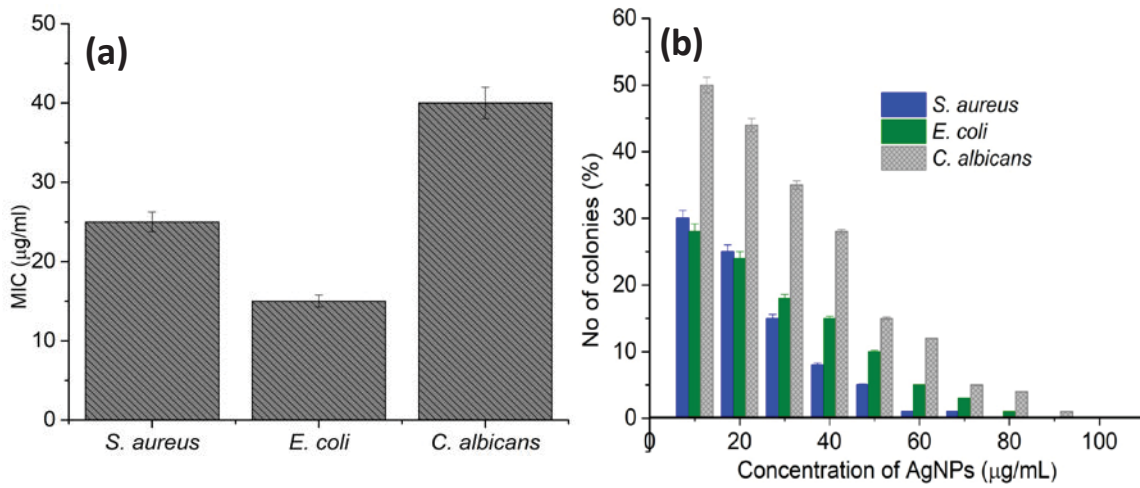


Fig. 3. (a) MIC of AgNPs against *S. aureus*, *E. coli* and *C. albicans* and (b) the number of colonies as a function of the concentration of AgNPs (µg/mL).

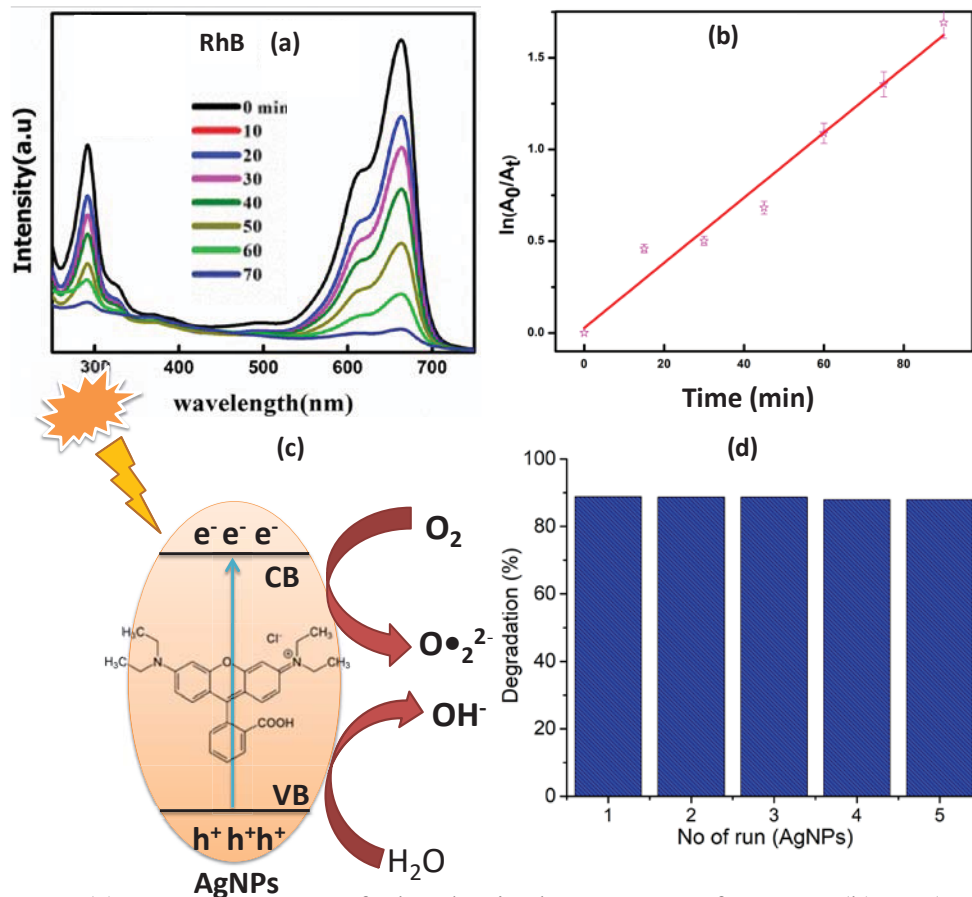


Fig. 4. (a) UV-Vis spectra of RhB dye in the presence of AgNPs, (b) $\ln(A_0/A_t)$ Vs time plot, (c) the mechanistic view of dye degradation in the presence of AgNPs and (d) RhB dye degradation activity of AgNPs up to 5 runs.

Tables:

Table 1. Zone of Inhibition (mm) and MIC ($\mu\text{g}/\text{mL}$) of AgNPs synthesized from *M. indica* bark extract for tested strains.

Test pathogens	AgNPs (50 $\mu\text{g}/\text{ml}$)	Standard (Ciprofloxacin/ Fluconazole)	Negative control (DMSO)	MIC ($\mu\text{g}/\text{ml}$)
	Zone of inhibition (in mm)			
<i>S. aureus</i>	15.37 \pm 0.34	24	No Inhibition	25
<i>E. coli</i>	18.47 \pm 0.47	25	No Inhibition	15
<i>C. albicans</i>	11.23 \pm 0.27	17	No Inhibition	40

Table 2. Comparison of the antimicrobial activity of AgNPssynthesized using different plant parts

Different plant extract (leaves, bark, seeds)	Test strains	Zone of Inhibition (mm)	Reference
<i>Solanum tricobatum</i> leaves extract	<i>S. aureus</i>	17.0	27
	<i>E. coli</i>	8.00	
<i>Banana peel</i> extract	<i>C. albicans</i>	10.10	28
<i>Impatiens balsamina</i> leaves extract	<i>S. aureus</i>	11.03	30
	<i>E. coli</i>	10.20	
<i>Terminalia Arjuna</i> bark extract	<i>S. aureus</i>	8.00	29
	<i>E. coli</i>	11.00	
	<i>C. albicans</i>	06.00	
<i>Dioscorea batatas</i> rhizome extract	<i>C. albicans</i>	10.00	31
<i>Withaniasomnifera</i> leaves extract	<i>S. aureus</i>	11.00	32

	<i>C. albicans</i>	No Inhibition	
<i>M. indica</i> bark	<i>S. aureus</i>	15.37	<i>Present study</i>
	<i>E. coli</i>	18.47	
	<i>C. albicans</i>	11.23	

Acknowledgment

The authors thank the Environmental Research Laboratory, Indian Institute for Human Settlement, Bangalore, for conducting this research.

References

1. S. Sultana and M. Ilyas, *Phytochemistry* 25, 953, 1986.
2. D. T. M. Huonga, L. T. Anh, N. T. Cuc, N. X. Nhiem, B. H. Tai, P. Van Kiem, M. Litaudon, T. D. Thach, C. Van Minh, and V. C. Pham, *Phytochem. Lett.* 34, 39, 2019.
3. L. T. N. Vu, L. T. Anh, N. T. Cuc, N. X. Nhiem, B. H. Tai, P. Van Kiem, M. Litaudon, T. D. Thach, C. Van Minh, and H. D. T. Mai, *Nat. Prod. Res.* 35, 2123, 2021.
4. J. M. Joseph, *J. Med. Plants Res.* 8, 489, 2014.
5. S. Sultana and M. Ilyas, CHEMICAL INVESTIGATION OF MACARANGA-INDICA WIGHT, 1987.
6. M. T. Wingo, J. M. Huber, J. H. Szostek, S. L. Bornstein, J. A. Post, K. F. Mauck, and M. L. Wieland, *Am. J. Med.* 134, 854, 2021.
7. M. Shivakumar, K. L. Nagashree, S. Yallappa, S. Manjappa, K. S. Manjunath, and M. S. Dharmaprakash, *Enzyme Microb. Technol.* 97, 55, 2017.
8. S. Yallappa, J. Manjanna, S. K. Peethambar, A. N. Rajeshwara, and N. D. Satyanarayan, *J. Clust. Sci.* 24, 1081, 2013.
9. D. Hebbalalu, J. Lalley, M. N. Nadagouda, and R. S. Varma, *ACS Sustain. Chem. Eng.* 1, 703, 2013.
10. T. K. Dua, S. Giri, G. Nandi, R. Sahu, T. K. Shaw, and P. Paul, *Food Chem. Adv.* 100205, 2023.
11. N. T. T. Nguyen, L. M. Nguyen, T. T. T. Nguyen, R. K. Liew, D. T. C. Nguyen, and T. Van Tran, *Sci. Total Environ.* 154160, 2022.
12. C. Singh, S. K. Anand, R. Upadhyay, N. Pandey, P. Kumar, D. Singh, P. Tiwari, R. Saini, K. N. Tiwari, and S. K. Mishra, *Mater. Chem. Phys.* 127413, 2023.
13. T. Fazal, A. Razzaq, F. Javed, A. Hafeez, N. Rashid, U. S. Amjad, M. S. U. Rehman, A. Faisal, and F. Rehman, *J. Hazard. Mater.* 390, 121623, 2020.
14. S. Joseph and B. Mathew, *Mater. Sci. Eng. B* 195, 90, 2015.
15. D. Gola, N. Bhatt, M. Bajpai, A. Singh, A. Arya, N. Chauhan, S. K. Srivastava, P. K. Tyagi, and Y. Agrawal, *Curr. Res. Green Sustain. Chem.* 4, 100132, 2021.
16. Y. Y. Loo, Y. Rukayadi, M. A. R. Nor-Khaizura, C. H. Kuan, B. W. Chieng, M. Nishibuchi, and S. Radu, *Front. Microbiol.* 9, 1, 2018.
17. P. Lodeiro, E. P. Achterberg, J. Pampín, A. Affatati, and M. S. El-Shahawi, *Sci. Total Environ.* 539, 7, 2016.

18. Hemlata, P. R. Meena, A. P. Singh, and K. K. Tejavath, *ACS omega* 5, 5520, 2020.
19. S. Chouhan and S. Guleria, *Mater. Sci. Energy Technol.* 3, 536, 2020.
20. D. Baruah, R. N. S. Yadav, A. Yadav, and A. M. Das, *J. Photochem. Photobiol. B Biol.* 201, 111649, 2019.
21. M. S. Mehata, *Chem. Phys. Lett.* 778, 138760, 2021.
22. F. A. Qais, A. Shafiq, H. M. Khan, F. M. Husain, R. A. Khan, B. Alenazi, A. Alsalmeh, and I. Ahmad, *Bioinorg. Chem. Appl.* 2019 2019.
23. D. Thatikayala, N. Jayarambabu, V. Banothu, C. B. Ballipalli, J. Park, and K. V. Rao, *J. Mater. Sci. Mater. Electron.* 30, 17303, 2019.
24. A. Chakravarty, I. Ahmad, P. Singh, M. U. D. Sheikh, G. Aalam, S. Sagadevan, and S. Ikram, *Chem. Phys. Lett.* 795, 139493, 2022.
25. F. Al-Otibi, S. K. Alkhudhair, R. I. Alharbi, A. A. Al-Askar, R. M. Aljowaie, and S. Al-Shehri, *Molecules* 26, 6081, 2021.
26. P. A. Lambert, *J. Appl. Microbiol.* 92, 46S, 2002.
27. P. Logeswari, S. Silambarasan, and J. Abraham, *J. Saudi Chem. Soc.* 19, 311, 2015.
28. H. M. M. Ibrahim, *J. Radiat. Res. Appl. Sci.* 8, 265, 2015.
29. S. Yallappa and J. Manjanna, *J. Clust. Sci.* 25, 1449, 2014.
30. H. F. Arintonang, H. Koleangan, and A. D. Wuntu, *Int. J. Microbiol.* 2019 2019.
31. K. D. Lee and P. C. Nagajyothi, *J. Nanomater.* 2011 2011.
32. R. W. Raut, V. D. Mendhulkar, and S. B. Kashid, *J. Photochem. Photobiol. B Biol.* 132, 45, 2014.
33. F. Hossain, O. J. Perales-Perez, S. Hwang, and F. Román, *Sci. Total Environ.* 466, 1047, 2014.
34. S. Rajendran, A. Mukherjee, T. A. Nguyen, C. Godugu, and R. K. Shukla, *Nanotoxicity: prevention and antibacterial applications of nanomaterials*, Elsevier (2020).
35. K. Rokesh, S. C. Mohan, S. Karuppuchamy, and K. Jothivenkatachalam, *J. Environ. Chem. Eng.* 6, 3610, 2018.
36. K. Roy, C. K. Sarkar, and C. K. Ghosh, *Spectrochim. Acta Part A Mol. Biomol. Spectrosc.* 146, 286, 2015.
37. W. Liang, T. L. Church, and A. T. Harris, *Green Chem.* 14, 968, 2012.
38. H. Veisi, S. Azizi, and P. Mohammadi, *J. Clean. Prod.* 170, 1536, 2018.